TELKOMNIKA Telecommunication Computing Electronics and Control
Vol. 24, No. 4, August 2026, pp. 1342~1352
ISSN: 1693-6930, DOI: 10.12928/TELKOMNIKA.v24i4.27726

A vector-valued PDE model unifying anisotropic diffusion and shock filter for color images denoising and deblurring

Said Karoui[1,2], Salim Bettahar[1,3]
[1]Department of Electronics, Faculty of Electronics and Electrical Engineering, University of Sciences and Technology of Oran Mohamed Boudiaf, Oran, Algeria
[2]Intelligent Systems Research Laboratory (LARESI), University of Sciences and Technology of Oran Mohamed Boudiaf, Oran, Algeria
[3]Electrical Engineering Laboratory of ORAN, University of Sciences and Technology of Oran Mohamed Boudiaf, Oran, Algeria

Article Info

Article history:

Received Dec 16, 2025
Revised Apr 14, 2026
Accepted May 25, 2026

Keywords:

Blur
Color
Diffusion
Noise
Shock filter

ABSTRACT

This paper proposes a novel and efficient method for the restoration of color images degraded by the combined effects of noise and blur. To address this challenging inverse problem, a mixed partial differential equation (PDE) model based on a semi-implicit numerical scheme is developed for color image restoration. The proposed approach integrates anisotropic diffusion and shock filtering within a unified vector-valued framework, allowing the different color channels to be processed jointly while preserving their mutual correlation. This formulation enables selective smoothing that efficiently suppresses noise in homogeneous regions while simultaneously enhancing and preserving significant edge and structural features. Extensive experimental results on various color images demonstrate that the proposed method consistently outperforms existing color image restoration techniques. Quantitative evaluations based on standard image quality assessment metrics, including peak signal-to-noise ratio (PSNR) and structural similarity index (SSIM), confirm the superior restoration performance of the proposed approach. Furthermore, the proposed model maintains chromatic consistency across color channels during simultaneous denoising and deblurring, effectively preventing the introduction of color artifacts and ensuring visually faithful restoration results. The numerical implementation of the proposed method is based on a semi-implicit scheme.

Corresponding Author:

Said Karoui
Intelligent Systems Research Laboratory (LARESI), University of Sciences and Technology of Oran Mohamed Boudiaf, Oran, Algeria
Email: said.karoui@univ-usto.dz

1. INTRODUCTION

Partial differential equation (PDE)-based methods have demonstrated notable efficacy as tools for image restoration, offering various solutions to address challenges such as noise interference and low resolution inherent in acquired images. Extensive exploration within this domain has led to the development of numerous PDE-based techniques. Notably, edge sharpening elliptic methods are commonly associated to shock filters [1], whereas selective smoothing models deal with anisotropic diffusion [2]–[4], fourth order methods [5]–[7], fractional diffusion methods [8]–[10] and PDE-based variational approach [11]–[13].

To address the restoration of degraded images afflicted by both noise and blur, several PDE-based techniques have been proposed, particularly for grayscale images, where diffusion is coupled with shock filters [14]–[19]. This dual approach leverages diffusion to mitigate noise in homogeneous regions while employing shock filters to enhance resolution through deblurring operations. However, the extension of such methods to color images has been relatively scarce [20]–[22], primarily due to the intricate interplay among different color components, which poses challenges in effectively combining anisotropic diffusion and shock filtering without introducing undesirable artifacts such as false colors artifacts. To overcome these challenges, the development of vectorial methods tailored to the nuances of color images is imperative. This paper presents a novel vectorial approach based on a semi-implicit numerical scheme that couples diffusion with a shock filter to effectively denoise and sharpen color images afflicted by noise and blur simultaneously, all while mitigating the risk of introducing color artifacts. Figure 1 shows the basic flow for denoising and deblurring color images. The approach is applicable to a wide range of image restoration tasks, including the digital restoration of degraded color documents, enhancement of consumer photographs affected by sensor noise and slight motion or defocus blur, medical color imaging where images are often noisy and blurred, satellite and aerial imaging subject to atmospheric degradation, surveillance and security systems operating under poor lighting conditions, as well as underwater and low-illumination environments.

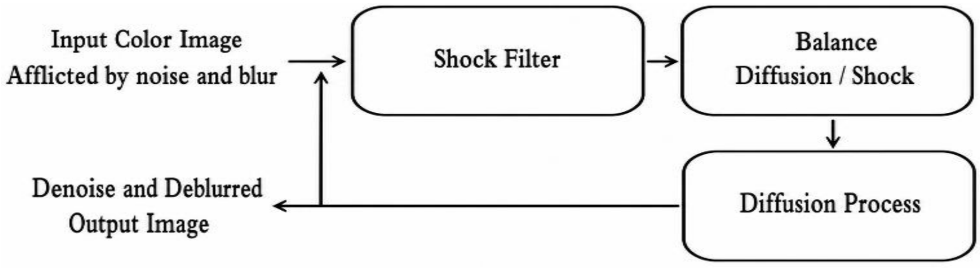

Figure 1. Flow based approach for denoising and blurring color images

2. RELATED WORKS

Tschumperlé and Deriche [20] introduced a diffusion-shock filter coupling mechanism incorporating a reactive term. This model considers the correlation among all color components within an image by employing two novel directions [23], where diffusion and shock terms are computed using shared directions across all image components. The model uses decreasing functions of the common gradient magnitude, which is computed using the Di Zenzo norm [23]. The proposed filter yields satisfactory outcomes by effectively reducing noise and improving the quality of color images. Nevertheless, despite its use of a vector-based approach, the shock filter may still produce erroneous colors in certain instances [21].

Bettahar *et al*. [21] subsequently developed a vectorial diffusion-shock filter coupling model specifically tailored for color image enhancement. This model incorporates single vectors representing the gradient magnitude and second derivatives to establish connections among various color components within the image. In the Bettahar filter, a nonlinear reaction-curvature diffusion process is employed. The model is composed of two terms: the first ensures selective smoothing that reduces noise in homogeneous regions of the image, while the second corresponds to a simple shock filter [21].

On the other hand, to denoise and deblur low-resolution images, Xiao *et al*. [22] introduced a novel approach for image super-resolution and enhancement. To ensure the smoothness and effectiveness of the shock filter at image edges, Xiao's model combines an edge-stopping function with a forward diffusion process. It is important to note that in [22], the authors addressed the problem of color image processing without comparing their method to the most relevant PDE-based algorithms for color images [20], [21]. Instead, their focus was on marginal variations of existing methodologies, which are known to be inefficient for color images [21].

3. PROPOSED MODEL

To advance the efficacy of shock filter-diffusion coupling schemes for color image sharpening and denoising, we introduce a model designed to efficiently enhance edges while removing noise, drawing upon prior methodologies, and preserving the integrity of shock locations. Our approach amalgamates modified curvature diffusion with a shock filter. The model is founded upon the following principles:

$$\begin{cases} {u_p}_t = |\nabla u| \, div \, \left(g\,(|\nabla u_\sigma|)\, \frac{\nabla u_p}{|\nabla u|} \right) - \alpha \left(\text{Max-}g\,(|\nabla u_\sigma|) \right) \left(u_p - v_p \right) \\ {v_p}_t = -sign \, \left(G_\sigma * u_{\eta\eta} \right) \, |\nabla u_p| \end{cases} \tag{1}$$

where $v_p(t)$ denotes the the immediately preceding value of the component $u_p(t)$, the index $p = 1,2,3$ corresponds red, green and blue color respectively of the restored image, and $u_p(0) = u_{p_O}$ is the input image referring to the component p and $v_p(0) = v_{p_O}$. The symbol $*$ denotes the convolution operator; G_σ is the Gaussian function with the standard deviation $\sigma$and u_σ is the smooth version of the image u using the Gaussian kernel. The parameter α is a constant that highlights the balance between the diffusion process and the schoc filter. $u_{\eta\eta}$ is the second derivative of the image in the gradient direction η. $g(|\nabla u_\sigma|)$ is a decreasing function of gradient magnitude ($|\nabla u|$) of the smooth image u_σ.

$$g(\,|\nabla u_\sigma|\,) = \frac{1}{1+\frac{|\nabla u_\sigma|^2}{K^2}} \tag{2}$$

where the constant K is a parameter that controls the degree of the smoothing. Max is the maximum value of $g(|\nabla u_\sigma|)$ in the neighbour of a given pixel.

To analyze the correlation among all components of the color image, while also considering the individual behaviour of each component, the proposed model employs two different approaches for computing the gradient norm. A marginal approach is used to compute the gradient ($\nabla u_{p)}$ in the divergence function and the shock filter terms, while a common vector norm $|\nabla u|$ is utilized to estimate the gradient magnitude of the smoothed version of the color image by using Di Zenzo norm:

$$|\nabla u| = \sqrt{\sum_{p=1}^{3} \left|\nabla u_p\right|^2} \tag{3}$$

Furthermore, to ensure a closer relationship among all components, we estimate the smoothed second derivative $u_{\eta\eta}$ in the computation of the *sign* function as follows:

$$u_{\eta\eta} = \sum_{p=1}^{3} u_{p_{\eta\eta}} \tag{4}$$

$$u_{p_{\eta\eta}} = \frac{u_{p_{xx}} u_{p_x}^2 + 2u_{p_{xy}} u_{p_x} u_{p_y} + u_{p_{yy}} u_{p_y}^2}{u_{p_x}^2 + u_{p_y}^2} \tag{5}$$

The term $\alpha(Max - g(|\nabla u_\sigma|))$ represents a balance between the diffusion process and the shock filter producing selectively smoothed regions and sharpened edges with $(u_{p-}v_p)$ as a reactive term. Initially, the value of v_p is computed using the second equation; subsequently, v_p is introduced in the first equation. Consequently, within stationary color regions, the gradient norm $|\nabla u_\sigma|$ is weak, yielding a value that tends towards 1 to the function $g(|\nabla u_\sigma|)$. In this case, $\alpha(Max - g(|\nabla u_\sigma|))$ tends towards 0 and shock filter effect is suppressed. Diffusion term then smooths noise across all image components using shared vectors. In the case of edges, $\alpha(Max - g(|\nabla u_\sigma|))$ takes value tending toward Max and the difference $(u_{p-}v_p)$ will be amplified by this factor. As a result, shocks are generated according to the magnitude of $|\nabla u_\sigma|$. Therefore, the process functions as diffusion filter in smooth regions, eliminating noise, and as a shock filter at region boundaries, enhancing edges without introducing color artifacts.

4. NUMERICAL IMPLEMENTATION

Finite difference schemes are employed to compute the required derivatives. Thus for values of p equal to 1, 2, and 3, the discrete image u_p is represented as a vector $[1 \times MN]$, where the components u_{pi}, $i \in [1, \dots, MN]$ correspond to the gray-level intensity at the respective pixels. Each pixel i associated with a spatial location x_i. Let h denote the discretization grid size. Discrete times $t_k = \tau k$ are employed, where k is a positive integer that determines the number of iterations and τ is the time step. ${u_p}_i^k$, ${v_p}_i^k$, $\left|\nabla u_p\right|_i^k$, $|\nabla u|_i^k$, $|\nabla u_\sigma|_i^k$, g_i^k,Max_i^k, $\left(u_{p_{\eta\eta}}^k\right)_i$, $\left(u_{\eta\eta}^k\right)_i$, and $sign_i^k$ denote approximations of $u_p(x_i, t_k)$, $v_p(x_i, t_k)$, $\left|\nabla u_p\right|$, $|\nabla u|$, $|\nabla u_\sigma|$, $g(|\nabla u_\sigma|)$, Max, $u_{p_{\eta\eta}}$, $u_{\eta\eta}$, and $sign(G_\sigma * u_{\eta\eta})$ respectively.

In the context of implementing temporal derivatives concerning component p, the following numerical schemes are adopted:

$$u_{p_t} = \frac{{u_p}^{k+1} - {u_p}^k}{\tau} \tag{6}$$

$$v_{p_t} = \frac{v_p{}^{k+1} - v_p{}^k}{\tau} \tag{7}$$

Firstly, we compute the second equation in the proposed model:

$$\frac{v_{p_i}^{k+1} - v_{p_i}^{k}}{\tau} = -\, sign_i^k \, \left|\nabla\, u_p\right|_i^k \tag{8}$$

As mentioned in the methodology, v_p is the previous value of u_p. it follows that:

$$\frac{v_{p_i}^{k+1} - v_{p_i}^{k}}{\tau} = -\, sign\,_i^k \, \left|\nabla\, u_p\right|_i^k \tag{9}$$

Subsequently, we are able to establish:

$$v_{p_i}^{k+1} = u_{p_i}^{k} - \tau\, sign\,_i^k \, \left|\nabla\, u_p\right|_i^k \tag{10}$$

During each iteration, the image $v_{p_i}^{k+1}$ will be injected into the first equation within the proposed model. For the implementation of $|\nabla u_p|$ in the shock equation, we use the following scheme:

$$\left|\nabla u_p\right|_i^k = \frac{1}{h}\sqrt{\left(m\left(\delta_+^x\, u_{p_i}^k, \delta_-^x\, u_{p_i}^k\right)\right)^2 + \left(m\left(\delta_+^y\, u_{p_i}^k, \delta_-^y\, u_{p_i}^k\right)\right)^2} \tag{11}$$

where δ_-^x and δ_+^x are backward and forward differences of $u_{p_i}^k$ in x direction and δ_-^y and δ_+^y are backward and forward differences of $u_{p_i}^k$ in y direction. $m(a,b)$ is the minmod function:

$$m(a,b) = \begin{cases} sign\,(a)\; min\;\; (|\,a\,|\,,|\,b\,|) & \text{if } ab > 0 \\ 0 & \text{otherwise} \end{cases} \tag{12}$$

For the discretisation of the second derivative $u_{p_{\eta\eta}}$, we use central differences to discretize all derivatives such as:

$$u_{p_{\eta\eta}} = \frac{u_{p_{xx}}^k \left(u_{p_x}^k\right)^2 + 2\, u_{p_{xy}}^k\, u_{p_x}^k\, u_{p_y}^k + u_{p_{yy}}^k \left(u_{p_y}^k\right)^2}{\left(u_{p_x}^k\right)^2 + \left(u_{p_y}^k\right)^2} \tag{13}$$

On the other hand, a semi-implicit scheme with harmonic averaging is used to approximate the quasi-divergence term [18], [24]:

$$|\nabla u|\; div\left(g\,(\,|\nabla u_\sigma|\,)\,\frac{\nabla\, u_p}{|\nabla u_\sigma|}\right) = |\nabla u|_i^k \sum_{j\in w(i)} \frac{2}{\left(\frac{|\nabla u_\sigma|_j^k}{g_j^k}\right) + \left(\frac{|\nabla u_\sigma|_i^k}{g_i^k}\right)}\; \frac{\left(u_{p_j}^k - u_{p_i}^k\right)}{h^2} \tag{14}$$

$w(i)$ consists of the four neighbours pixels of pixel i and

$$|\nabla u|_i^k = \sqrt{\sum_{l\in\{x,y\}} \sum_{p=1}^3 \left(\left|\nabla u_{p_l}\right|_i^k\right)^2} \tag{15}$$

$$|\nabla u_\sigma|_i^k = \sqrt{\sum_{l\in\{x,y\}} \sum_{p=1}^3 \left(\left|\nabla u_{\sigma_{p_l}}\right|_i^k\right)^2} \tag{16}$$

$$g_i^k = \frac{1}{1 + \left(\frac{|\nabla u_\sigma|_i^k}{k_d}\right)^2} \tag{17}$$

Taking into account that ${v_p}_i^k = {u_p}_i^k$, we can obtain the numerical scheme:

$$\frac{{u_p}_i^{k+1} - {u_p}_i^k}{\tau} = |\nabla u|_i^k \sum_{j\in w(i)} \frac{2}{\left(\frac{|\nabla u_\sigma|_j^k}{g_j^k}\right)+\left(\frac{|\nabla u_\sigma|_i^k}{g_i^k}\right)} \frac{\left({u_p}_j^k - {u_p}_i^k\right)}{h^2} - \alpha\left(Max_i^k - g_i^k\right)\left({u_p}_i^{k+1} - {u_p}_i^k + \tau\, sign_i^k \left|\nabla u_p\right|_i^k\right) \quad (18)$$

Thus

$$\begin{aligned} {u_p}_i^{k+1} &= \tau \frac{|\nabla u|_i^k}{h^2} \sum_{j\in w(i)} \frac{2}{\left(\frac{|\nabla u_\sigma|_j^k}{g_j^k}\right)+\left(\frac{|\nabla u_\sigma|_i^k}{g_i^k}\right)} {u_p}_j^{k+1} \\ &- \tau\left(\frac{|\nabla u|_i^k}{h^2} \sum_{j\in w(i)} \frac{2}{\left(\frac{|\nabla u_\sigma|_j^k}{g_j^k}\right)+\left(\frac{|\nabla u_\sigma|_i^k}{g_i^k}\right)} + \alpha\left(Max_i^k - g_i^k\right)\right) {u_p}_i^{k+1} \\ &+ \left(1 + \tau\alpha\left(Max_i^k - g_i^k\right)\right) {u_p}_i^k - \tau^2\alpha\left(Max_i^k - g_i^k\right) sign_i^k \left|\nabla u_p\right|_i^k \end{aligned} \quad (19)$$

Therefore, by using the matrix-vector notation [3], [18], we can obtain at each iteration k the solution u_p^{k+1} from the following semi-implicit scheme:

$$u_p^{k+1} = \tau A\left(u^k\right) u_p^{k+1} + \left(I + \tau\alpha B\left(u^k\right)\right) u_p^k - \tau^2 \alpha B\left(u^k\right) Sgn\left(u^k\right) \left|\nabla u_p\right|^k \quad (20)$$

Consequently, by decomposing the matrix A into x and y directions, the following expression is deduced:

$$\left(I - \tau \sum_{l\in\{x,y\}} A_l\left(u^k\right)\right) u_p^{k+1} = \left(\left(I + \tau\alpha B\left(u^k\right)\right) u_p^k - \tau^2 \alpha B\left(u^k\right) Sgn\left(u^k\right) \left|\nabla u_p\right|^k\right) \quad (21)$$

I denotes the unit matrix. The matrix A_l ($l \in \{x, y\}$), B and Sgn have components which are provided as follows:

$$\hat{a}_{ijl}\left(u^k\right) = \begin{cases} \frac{|\nabla u|_i^k}{h^2} \frac{2}{\left(\frac{|\nabla u_\sigma|_j^k}{g_j^k}\right)+\left(\frac{|\nabla u_\sigma|_i^k}{g_i^k}\right)} & j \neq i, j \in w_l(i) \\ -\frac{|\nabla u|_i^k}{h^2} \sum_{m\in w_l(i)} \frac{2}{\left(\frac{|\nabla u_\sigma|_j^k}{g_j^k}\right)+\left(\frac{|\nabla u_\sigma|_i^k}{g_i^k}\right)} - \alpha\left(Max_i^k - g_i^k\right) & j = i \\ 0 & \text{otherwise} \end{cases} \quad (22)$$

$w_l(i)$ represents the two neighbouring pixels with respect to the direction ($l \in \{x, y\}$).

$$\hat{b}_{ij}\left(u^k\right) = \begin{cases} Max_i^k - g_i^k & i = j \\ 0 & \text{otherwise} \end{cases} \quad (23)$$

$$\hat{s}_{ij}\left(u^k\right) = \begin{cases} sign_i^k & i = j \\ 0 & \text{otherwise} \end{cases} \quad (24)$$

However, the solution cannot be directly determined from the (20). Instead, it requires solving a linear system of equations. Its solution is formally expressed as:

$$u_p^{k+1} = \left(I - \tau \sum_{l\in\{x,y\}} A_l\left(u^k\right)\right)^{-1} \left(\left(I + \tau\alpha B\left(u^k\right)\right) u_p^k - \tau^2 \alpha B\left(u^k\right) Sgn\left(u^k\right) \left|\nabla u_p\right|^k\right) \quad (25)$$

It is notable that the matrix expressed as:

$$M = \left(I - \tau \sum_{l\in\{x,y\}} A_l \left(u^k\right)\right) \quad (26)$$

is invertible, because it is strictly diagonally dominant. i.e.,

$$| \mathrm{m}_{ii} | \succ \sum_{j\neq i} \left| \mathrm{m}_{ij} \right| \quad (27)$$

5. RESULTS AND COMPARISON

A performance comparison is conducted between the proposed model and the methods of Tschumperlé-Deriche, Xiao, and Bettahar. Parameter selection is guided to achieve optimal results for each filter. The values of these parameters are detremined empirically. The number of iterations is determined according to visual quality assessment, and, for each test image, the same number of iterations is used across all methods to ensure a fair comparison. Regarding the time step τ, a small value is chosen to improve precision while preserving fine details in the restored images. All models are applied to blurred and noisy images. Artificial blur is introduced via Gaussian convolution of the original test images, and noise is added by injecting random Gaussian noise into the blurred images. The implementation was carried out using the Python programming language on a gaming personal computer (PC) with an Intel core i7-8750 central processing unit (CPU) operating at 2.20 Ghz. In Figures 2 to 7, subfigures (a) to (f) correspond to the original image, blurred and noisy image, image restored using the Tschumperlé-Deriche filter, image restored using the Bettahar filter, image restored using the Xiao filter, and image restored using the proposed filter, respectively. For objective evaluation, the peak signal-to-noise ratio (PSNR) and structural similarity index (SSIM) are employed [25].

Figure 2 depicts the window image after blurring and noise addition, resulting in a PSNR of 29.53 dB. For the proposed filter, the parameters are set to $\sigma = 1$, $K = 3$, $\alpha = 20$, and $\tau = 0.05$ with 100 iterations for all filters. All methods effectively smooth noise in homogeneous regions. However, the Tschumperlé-Deriche filter exhibits a slight edge enhancement with residual false colors at edge locations, while the Xiao model produces residual false piecewise-constant artefacts in smooth regions, leading to the loss of small details. In contrast, the proposed filter accurately preserves edges without introducing false colors, as illustrated by a portion of the window image in Figure 3. Additionally, both the proposed method and Bettahar model yield good results. However, the Xiao method distorts shapes (sheets and red flower) by curving them. The model performs smoothing by applying only the directional diffusion term perpendicular to the gradient to the image. Notably, the proposed method achieves a higher PSNR than the competing models, which is further confirmed by the MSSIM values in Table 1.

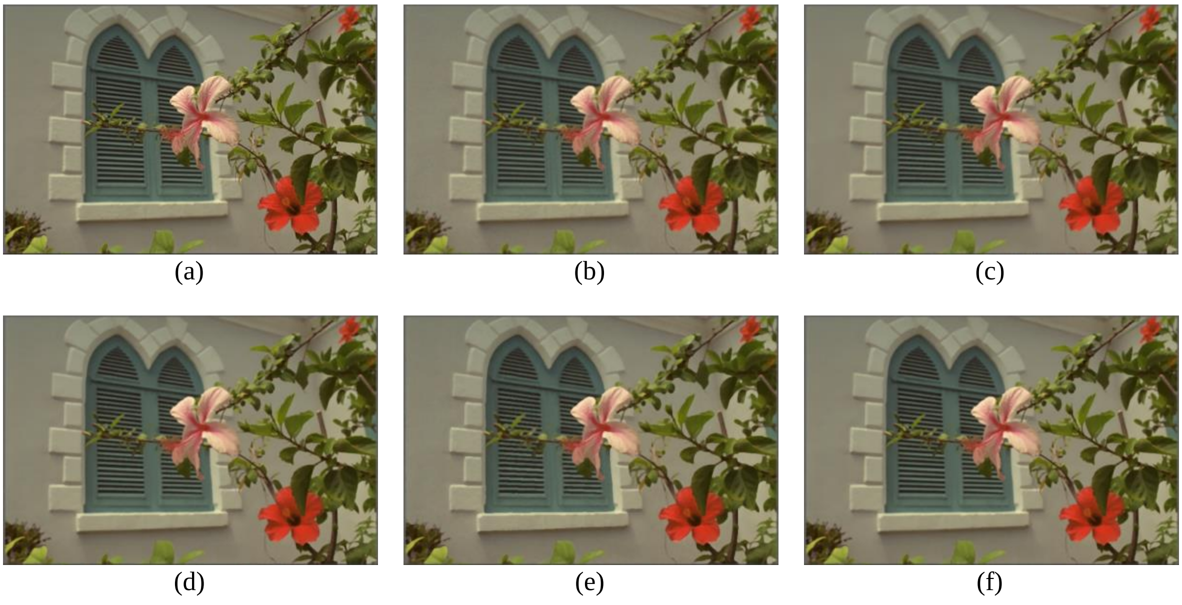

(a) (b) (c) (d) (e) (f)

Figure 2. Enhancement of window image: (a) original image, (b) blurry and noised image, (c) Tschumperlé-Deriche filter, (d) Bettahar filter, (e) Xiao filter, and (f) proposed filter

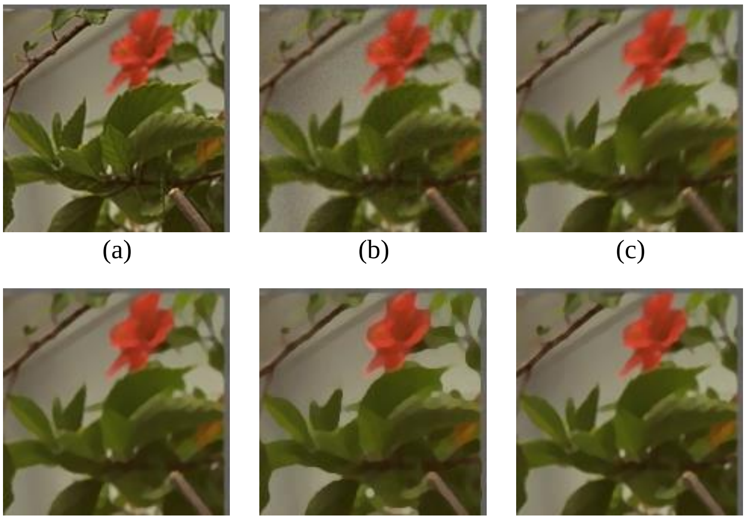

(a) (b) (c)

(d) (e) (f)

Figure 3. A part of window image: (a) original image, (b) blurry and noised image, (c) Tschumperlé-Deriche filter, (d) Bettahar filter, (e) Xiao filter, and (f) proposed filter

Table 1. The PSNR and SSIM for the various methods and the used images

	Tschumperlé-Deriche filter		Bettahar filter		Xiao filter		The proposed filter	
	PSNR	SSIM	PSNR	SSIM	PSNR	SSIM	PSNR	SSIM
Window	30.50	0.861	30.84	0.873	30.72	0.856	31.05	0.876
Face	35.59	0.858	35.75	0.859	35.19	0.851	35.80	0.862
Flowers	33.91	0.754	34.50	0.763	33.37	0.759	34.88	0.767

The second experiment considers the blurred and noisy face image, with an initial PSNR of 32.48 dB (Figure 4). The proposed filter the parameters are set to $\sigma = 1$, $K = 4$, $\alpha = 20$, and $\tau = 0.02$ with 200 iterations for all filters. While all models effectively reduce noise, closer inspection of local details (Figure 5) reveals notable differences. The Tschumperlé-Deriche method leaves residual false colors along the glass borders, whereas the Bettahar model produces a slimming effect on the white border of the cask. The Xiao method, by contrast, yields a cartoon-like appearance. The proposed approach efficiently enhances edges while smoothing noise in homogeneous regions, achieving the best PSNR and SSIM values among the compared methods (see Table 1).

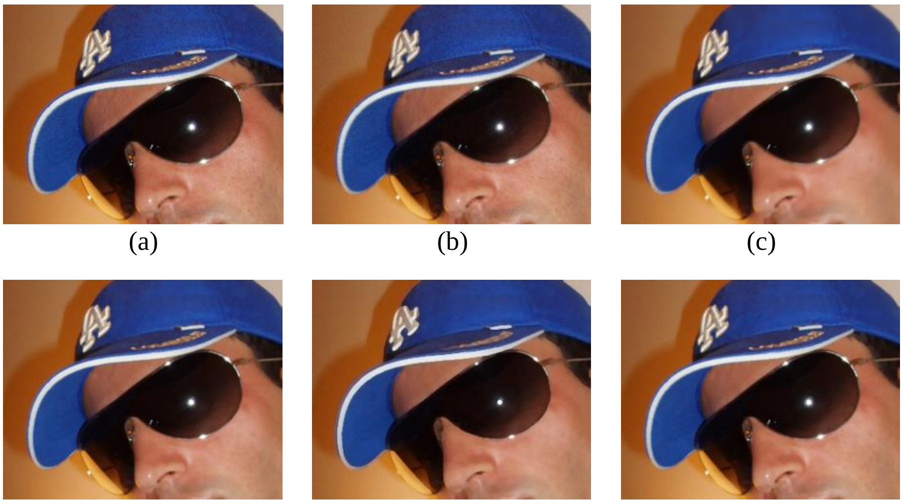

(a) (b) (c)

(d) (e) (f)

Figure 4. Enhancement of face image: (a) original image, (b) blurry and noised image, (c) Tschumperlé-Deriche filter, (d) Bettahar filter, (e) Xiao filter, and (f) proposed filter

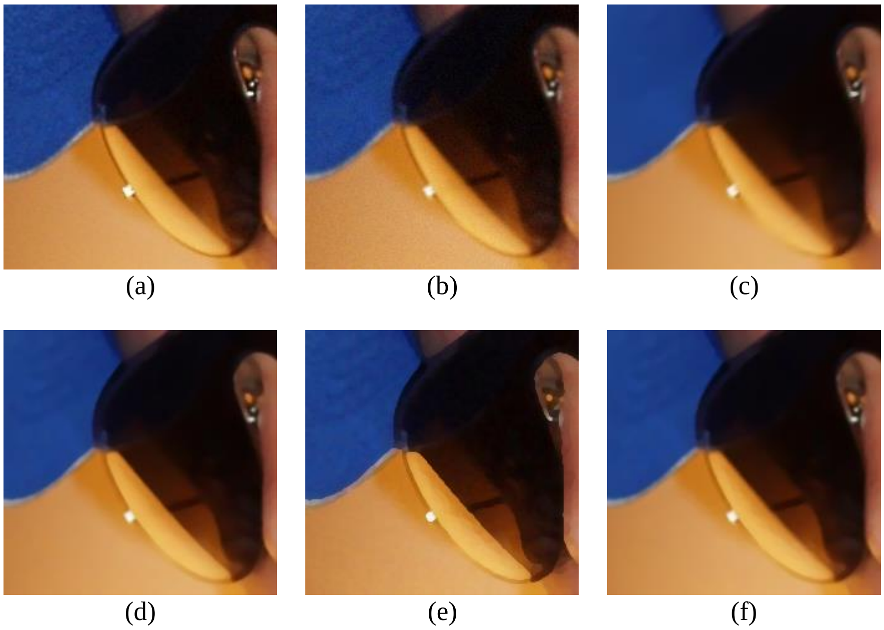

Figure 5. A part of face image: (a) original image, (b) blurry and noised image, (c) Tschumperlé-Deriche filter, (d) Bettahar filter, (e) Xiao filter, and (f) proposed filter

For further comparison, Figure 6 presents the flowers image after blurring and noise addition, with an initial PSNR of 31.71 dB. The proposed filter, uses the parameters $\sigma = 1$, $K = 4$, $\alpha = 40$, and $\tau = 0.02$ with 150 iterations for all filters. This experiment confirms the trends observed previously. As shown in Figure 7, the Tschumperlé-Deriche method introduces false colors along the borders of the yellow flower and the sheets, while the Xiao model distorts them by curving. Both the Bettahar and the proposed models deliver comparable visual quality, and outperform the Tschumperlé-Deriche and Xiao approaches. Nevertheless, the proposed filter achieves superior PSNR and SSIM values (see Table 1).

Figure 6. Enhancement of flowers image: (a) original image, (b) blurry and noised image, (c) Tschumperlé-Deriche filter, (d) Bettahar filter, (e) Xiao filter, and (f) proposed filter

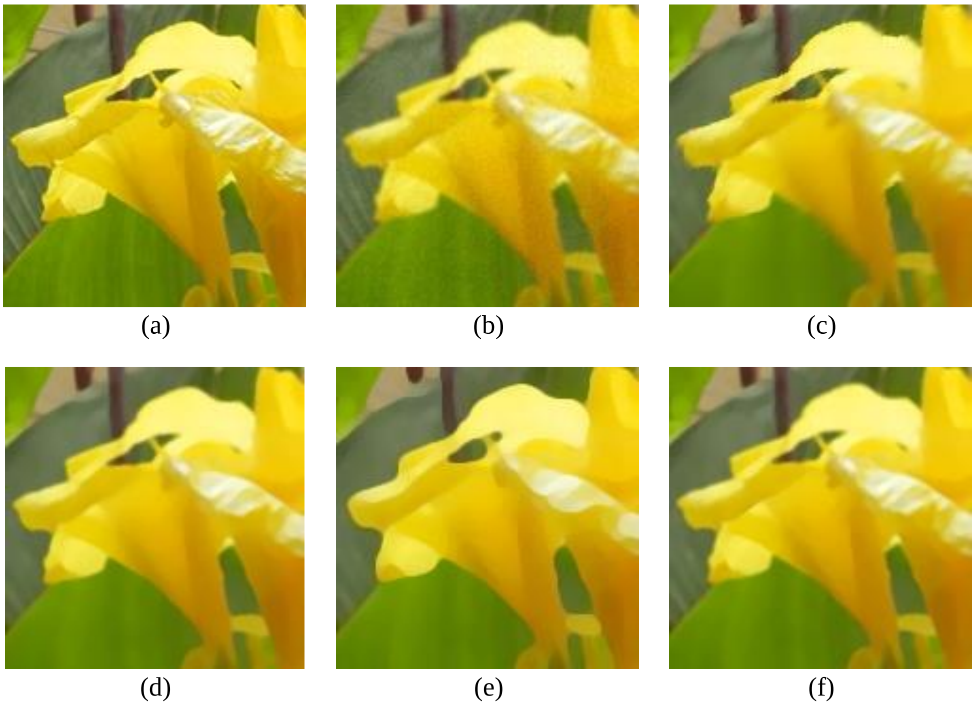

Figure 7. A part of flowers image: (a) original image, (b) blurry and noised image, (c) Tschumperlé-Deriche filter, (d) Bettahar filter, (e) Xiao filter, and (f) proposed filter

6. CONCLUSION

We propose a semi-implicit scheme that combines a shock filter with curvature-based diffusion for the simultaneous enhancement of color images degraded by noise and blur. The proposed model enables selective smoothing, effectively suppressing noise while preserving and sharpening edges. Experimental analysis demonstrates that the proposed method outperforms existing color image restoration approaches without introducing false color artifacts, achieving superior performance in terms of PSNR and SSIM. Despite these advantages, the semi-implicit scheme exhibits certain limitations. The performance of the model is sensitive to parameter selection, where inappropriate choices may result in insufficient noise removal or excessive edge sharpening. Moreover, the model parameters remain fixed during evolution and do not adapt to local image content, which may reduce robustness across diverse image types. The iterative solution of the underlying PDEs also incurs a relatively high computational cost, limiting applicability to real-time or large-scale scenarios. Future work will focus on incorporating adaptive and data-driven parameter selection strategies to improve robustness. The integration of explicit blur modeling and multi-scale processing is expected to enhance performance under severe degradation. Furthermore, hybrid PDE-variational and learning-assisted frameworks may further improve texture preservation, computational efficiency, and overall restoration quality under real-world conditions (e.g., real camera noise and motion blur).

FUNDING INFORMATION

This research was supported by the Electrical Engineering Laboratory of the University of Sciences and Technology of Oran.

AUTHOR CONTRIBUTIONS STATEMENT

This journal uses the Contributor Roles Taxonomy (CRediT) to recognize individual author contributions, reduce authorship disputes, and facilitate collaboration.

Name of Author	C	M	So	Va	Fo	I	R	D	O	E	Vi	Su	P	Fu
Said Karoui	✓	✓		✓	✓	✓	✓	✓	✓	✓	✓	✓	✓	✓
Salim Bettahar	✓	✓	✓	✓	✓	✓	✓	✓	✓	✓	✓	✓		

C : **C**onceptualization
M : **M**ethodology
So : **So**ftware
Va : **Va**lidation
Fo : **Fo**rmal analysis
I : **I**nvestigation
R : **R**esources
D : **D**ata Curation
O : Writing - **O**riginal Draft
E : Writing - Review & **E**diting
Vi : **Vi**sualization
Su : **Su**pervision
P : **P**roject administration
Fu : **Fu**nding acquisition

CONFLICT OF INTEREST STATEMENT

Authors state no conflict of interest.

DATA AVAILABILITY

The data that support the findings of this study are openly available at:

- https://doi.org/10.1109/MSP.2002.1028349
- https://doi.org/10.1016/j.jvcir.2016.06.015
- https://doi.org/10.1109/TIP.2011.2177844

REFERENCES

[1] S. Osher and L. I. Rudin, "Feature-oriented image enhancement using shock filters," *SIAM Journal on Numerical Analysis*, vol. 27, no. 4, pp. 919–940, Aug. 1990, doi: 10.1137/0727053.

[2] P. Perona and J. Malik, "Scale-Space and Edge Detection Using Anisotropic Diffusion," *IEEE Transactions on Pattern Analysis and Machine Intelligence*, vol. 12, no. 7, pp. 629–639, Jul. 1990, doi: 10.1109/34.56205.

[3] R. T. Whitaker and X. Xue, "Variable-conductance, level-set curvature for image denoising," *IEEE International Conference on Image Processing*, vol. 3, pp. 142–145, 2001, doi: 10.1109/icip.2001.958071.

[4] J. Weickert, "Coherence-enhancing diffusion filtering," *International Journal of Computer Vision*, vol. 31, no. 2, pp. 111–127, Apr. 1999, doi: 10.1023/a:1008009714131.

[5] K. M. Furati, M. Yousuf, and A. Q. M. Khaliq, "Fourth-order methods for space fractional reaction–diffusion equations with non-smooth data," *International Journal of Computer Mathematics*, vol. 95, no. 6–7, pp. 1240–1256, Jul. 2018, doi: 10.1080/00207160.2017.1404037.

[6] A. Siddig, Z. Guo, Z. Zhou, and B. Wu, "An image denoising model based on a fourth-order nonlinear partial differential equation," *Computers and Mathematics with Applications*, vol. 76, no. 5, pp. 1056–1074, Sep. 2018, doi: 10.1016/j.camwa.2018.05.040.

[7] Y. Wen, J. Sun, and Z. Guo, "A New Anisotropic Fourth-Order Diffusion Equation Model Based on Image Features for Image Denoising," *Inverse Problems and Imaging*, vol. 16, no. 4, pp. 895–924, 2022, doi: 10.3934/ipi.2022004.

[8] S. Kumar, K. Alam, and A. Chauhan, "Fractional derivative based nonlinear diffusion model for image denoising," *SeMA Journal*, vol. 79, no. 2, pp. 355–364, Jun. 2022, doi: 10.1007/s40324-021-00255-0.

[9] Q. Wang, J. Ma, S. Yu, and L. Tan, "Noise detection and image denoising based on fractional calculus," *Chaos, Solitons and Fractals*, vol. 131, p. 109463, Feb. 2020, doi: 10.1016/j.chaos.2019.109463.

[10] A. Annadurai, V. Sureshkumar, D. Jaganathan, and S. Dhanasekaran, "Enhancing Medical Image Quality Using Fractional Order Denoising Integrated with Transfer Learning," *Fractal and Fractional*, vol. 8, no. 9, p. 511, Aug. 2024, doi: 10.3390/fractalfract8090511.

[11] S. Osher, M. Burger, D. Goldfarb, J. Xu, and W. Yin, "An iterative regularization method for total variation-based image restoration," *Multiscale Modeling and Simulation*, vol. 4, no. 2, pp. 460–489, Jan. 2005, doi: 10.1137/040605412.

[12] T. Barbu, V. Barbu, V. Biga, and D. Coca, "A PDE variational approach to image denoising and restoration," *Nonlinear Analysis: Real World Applications*, vol. 10, no. 3, pp. 1351–1361, Jun. 2009, doi: 10.1016/j.nonrwa.2008.01.017.

[13] A. Wahid and H. J. Lee, "Image denoising method based on directional total variation filtering," in *International Conference on Information and Communication Technology Convergence: ICT Convergence Technologies Leading the Fourth Industrial Revolution, ICTC 2017*, IEEE, Oct. 2017, pp. 798–802. doi: 10.1109/ICTC.2017.8190785.

[14] L. Alvarez and L. Mazorra, "Signal and image restoration using shock filters and anisotropic diffusion," *SIAM Journal on Numerical Analysis*, vol. 31, no. 2, pp. 590–605, Apr. 1994, doi: 10.1137/0731032.

[15] P. Kornprobst, R. Deriche, and G. Aubert, "Image coupling, restoration and enhancement via PDE's," in *IEEE International Conference on Image Processing*, IEEE Comput. Soc, 1997, pp. 458–461. doi: 10.1109/icip.1997.638807.

[16] G. Gilboa, N. Sochen, and Y. Y. Zeevi, "Image enhancement and denoising by complex diffusion processes," *IEEE Transactions on Pattern Analysis and Machine Intelligence*, vol. 26, no. 8, pp. 1020–1036, Aug. 2004, doi: 10.1109/TPAMI.2004.47.

[17] S. Fu, Q. Ruan, W. Wang, and J. Chen, "Region-based shock-diffusion equation for adaptive image enhancement," in *Lecture Notes in Computer Science (including subseries Lecture Notes in Artificial Intelligence and Lecture Notes in Bioinformatics)*, 2006, pp. 387–395. doi: 10.1007/11821045_41.

[18] S. Bettahar and A. B. Stambouli, "Shock filter coupled to curvature diffusion for image denoising and sharpening," *Image and Vision Computing*, vol. 26, no. 11, pp. 1481–1489, Nov. 2008, doi: 10.1016/j.imavis.2008.02.010.

[19] C. Ludusan, O. Lavialle, R. Terebes, and M. Borda, "Morphological sharpening and denoising using a novel shock filter model," in *Lecture Notes in Computer Science (including subseries Lecture Notes in Artificial Intelligence and Lecture Notes in Bioinformatics)*, 2010, pp. 19–27. doi: 10.1007/978-3-642-13681-8_3.

[20] D. Tschumperlé and R. Deriche, "Diffusion PDEs on vector-valued images," *IEEE Signal Processing Magazine*, vol. 19, no. 5, pp. 16–25, Sep. 2002, doi: 10.1109/MSP.2002.1028349.

[21] S. Bettahar, A. B. Stambouli, P. Lambert, and A. Benoit, "PDE-based enhancement of color images in RGB space," *IEEE Transactions on Image Processing*, vol. 21, no. 5, pp. 2500–2512, May 2012, doi: 10.1109/TIP.2011.2177844.

[22] J. Xiao, G. Pang, Y. Zhang, Y. Kuang, Y. Yan, and Y. Wang, "Adaptive shock filter for image super-resolution and enhancement," *Journal of Visual Communication and Image Representation*, vol. 40, pp. 168–177, Oct. 2016, doi: 10.1016/j.jvcir.2016.06.015.

[23] S. Di Zenzo, "A note on the gradient of a multi-image," *Computer Vision, Graphics and Image Processing*, vol. 33, no. 1, pp. 116–125, Jan. 1986, doi: 10.1016/0734-189X(86)90223-9.

[24] J. Weickert, "Applications of nonlinear diffusion in image processing and computer vision," *Acta Math Univ Comenianae*, vol. LXX, no. 1, pp. 33–50, 2001, [Online]. Available: http://books.google.com/books?id=eSu5I9pU3rUC&pgis=1

[25] Z. Wang, A. C. Bovik, H. R. Sheikh, and E. P. Simoncelli, "Image quality assessment: From error visibility to structural similarity," *IEEE Transactions on Image Processing*, vol. 13, no. 4, pp. 600–612, Apr. 2004, doi: 10.1109/TIP.2003.819861.

BIOGRAPHIES OF AUTHORS

Said Karoui received a Bachelor's degree in Electrical Engineering from the University of Sciences and Technology of Oran (USTOMB), Algeria in 1988, and a Ph.D. degree from Grenoble National Institute of Technology (INPG), France in 1993. He subsequently held various R&D engineering positions in the aerospace, automotive, and telecommunications industries in the Montreal area for 10 years. Since 2005, he has been an Associate Professor at the Electronics Department, Electronics and Electrical Engineering Faculty, University of Sciences and Technology of Oran Mohamed Boudiaf. His research interests include circuits and system testing, design for EMI, design and reliability studies of space applications, signal and imange processing, and the design of embedded digital system. He can be contacted at email: said.karoui@univ-usto.dz.

Salim Bettahar received the Engineer Degree in Electronics in 1998, and the Degree of Magister and Ph.D. in 2002 and 2009 respectively in non-destructive testing and imaging. He is currently a full professor at the University of Sciences and Technology of Oran, Algeria. His research interest concerns the application of partial differential equations in image processing and computer vision. He is a member of the Electrical Engineering Laboratory of Oran, Algeria. He can be contacted at email: salim.bettahar@univ-usto.dz.